Available online at www.sciencedirect.com
SCIENCE DIRECT®
Journal of Sound and Vibration 279 (2005) 1037–1070
JOURNAL OF SOUND AND VIBRATION
www.elsevier.com/locate/jsvi

Dynamics of arm of a flat belt drive pulley with explanation of belt flutter

Pravin M. Singru[a,*], Jayant P. Modak[b]

[a] *Rajiv Gandhi College of Engineering, Research and Technology, Babupeth, Chandrapur, MS 442403, India*
[b] *Priyadarshini College of Engineering and Architecture, CRPF, Nagpur, India*

Received 7 April 2003; accepted 26 November 2003

Abstract

External force system acting on the pulley outer surface is non-linearly varying frictional force as produced by the belt on the pulley. This paper deals with dynamics of arm of belt drive pulley using unbalanced couple approach, by computer simulation, and with analysis of armload variation. Equilibrium of rim is considered assuming it as thin. The arm is subjected to varying load. The expression for the intensity of the frictional force per unit length of the arc of contact is found. This arc of contact is divided into angle of iteration taken at a time for analysis that is further sub-divided into number of divisions. Resultant frictional force is found by summing up the elemental frictional force coming on elemental portion of rim. Here an iterative algorithm is suggested to find armload variation. From equilibrium of this elemental portion of rim armload is calculated. There are two possible solutions of this equilibrium equation: (1) Resultant frictional force is passing through the tip of the arm at the arm–rim interface. (2) Resultant frictional force is not passing through the tip of the arm at the arm–rim interface, but somewhere away from it. In this case the arm has to supply some couple to maintain the equilibrium. When the arm is unable to provide or some other mechanism is unable to provide the reaction couple at arm–rim interface, there is momentary loss of contact between the belt and the rim, causing belt flutter. The stress under vibration is then calculated and compared with previous results. The results of this approach are more refined as compared with previous results.

1. Introduction

A flat belt drive is designed by limiting the maximum tension T_t according to the permissible tensile stress specified for the belt material [1–5]. Pulley material is generally cast iron or cast steel.

*Corresponding author.
E-mail addresses: pravinsingru@yahoo.com (P.M. Singru), jpmodak@yahoo.com (J.P. Modak).

0022-460X/$ - see front matter © 2003 Elsevier Ltd. All rights reserved.
doi:10.1016/j.jsv.2003.11.019

Pulleys with less than 100 mm diameters are like solid discs. A pulley with diameter less than 600 mm has 4 arms and for diameter more than 600 mm, has 6 arms. The cross section of arm is generally elliptical with major axis equal to twice the minor axis. Rectangular as well as circular cross-sections are sometimes used. The arms are checked to determine bending stress considering them to be cantilever beams fixed in the hub and carrying a concentrated load at the rim end. The length of cantilever is taken equal to radius of the pulley [6–9].

In case of driven pulley, it is assumed that, at any given time, the power is transmitted from the hub to the rim, through half the total number of arms [6–10]. The rim is not sufficiently thick that, it can distribute the load amongst all the arms and hence the assumption of only half the number of arms sharing the load equally is made. The belt tension variation over the angle of lap given by $T_t = T_s e^{\mu\varphi}$. The portion of pulley under the angle of lap is subjected to non-linearly varying frictional force and the arms changing their position every instant, gives a feeling that the assumption of equal load distribution amongst the arm seems unrealistic. In absence of information regarding load variation as a function of its position, rim thickness, pulley diameter, number of arms, loading conditions and material properties, the design of arm is based on this assumption [6–10]. Also it is difficult to visualize the range of thickness for which the thin rim assumption is realistic.

This practice is followed since a long time and failure of arms is not reported from industries. So the need was not felt to analyze this problem and prove the validity of this assumption. The above discussion created a need of developing mathematical model of armload variation as a function of, torque to be transmitted, number of arms, thickness of rim, diameter of pulley, properties of rim material, any other relevant parameter.

The model so evolved should be used to optimize the rim thickness to get desired load variation of the arm. But manufacturing consideration may force to keep the rim thickness above optimum. However, the model will be useful from the point of view of controlling armload variation. This pattern of load variation of arm will be useful in investigating the stress under vibration.

This paper deals with analysis of armload variation. Equilibrium of rim is considered assuming it as thin. The arm is subjected to varying load. The expression for the intensity of the frictional force per unit length of the arc of contact is found. This arc of contact is divided into angle of iteration taken at a time for analysis that is further subdivided into number of divisions. Resultant frictional force is found by summing up the elemental frictional force coming on elemental portion of rim. From equilibrium of this elemental portion of rim armload is calculated. There are two possible solutions of this equilibrium equation:

1. Resultant frictional force is passing through the tip of the arm at the arm–rim interface.
2. Resultant frictional force is not passing through the tip of the arm at arm–rim interface, but somewhere away from it. In this case the arm has to supply some couple to maintain the equilibrium. When the arm is unable to provide or some other mechanism is unable to provide the reaction couple at arm–rim interface, there is momentary loss of contact between the belt and the rim, causing belt flutter.

In this paper using equilibrium of rim, the force variation acting on the arms is calculated using an iterative algorithm. To find out response of the arm subjected to this load, an equivalent spring–mass–damper system is created and this forcing function is given to the system. The

variation of armload is highly non-linear which forced us to use the concept of impulse response. Converting the variation of force as series of impulses, we solved the equation of motion. Here free vibration case is considered, as we have to compare the results with previous results by Singru and Modak [12]. This work was first attempt to find dynamic and vibration response of pulleys of a flat belt drive. From this stress under vibration is found out. This approach of considering equilibrium of rim gave us more refined results over the previous approach and hence presented [12].

1.1. Literature review

Modak et al. suggested three approaches for the analysis of the armload variation exclusively for torque transmission from rim to the shaft through arms of the pulleys [11]:

1. Equal distribution of load zone by the arm based on highly simplified assumption.
2. Equilibrium of rim portion.
3. Qualitative analysis of a suggestion for an approach by finite element method.

Singru and Modak performed computer simulation of dynamic and vibration response of arms of flat belt pulleys on the basis of first of the above three approaches [12]. In this work, an idea of maximum stress under vibration and load variation of the arm of flat belt pulley is achieved. Abrate [13] reviewed the state-of-the-art in vibration analysis of power transmission belts. Models available for analyzing the free and forced vibrations of the belt are discussed. Vibrations of belt drives are also considered, and the influences of several complicating factors are mentioned. In this paper a need was stressed to model a complete belt drive and accounting for coupling between transverse belt vibration and pulley rotation.

Saraph [14] presented a three-dimensional finite element stress analysis of a sheave. Excellent co-relation of results is obtained between the results obtained by FEM and experimentation. These results indicate that all arms are subjected to different and varying loads. Belofsky [15] derived a new formulation for the tension ratio T_t/T_s in the creep regime from the quasi-static equilibrium equation and includes the effect of belt elasticity, flexural rigidity and varying coefficient of friction along the contact arc. A simplified solution is found by utilization of experimental slip measurements. It is suggested that the new theory is better able to explain belt behavior and is in accord with the limited available experimental data in the creep regime. Under these conditions, tangential stress is theoretically invariant with belt angle. For slip regime, one equation based on empirical data is proposed for T_t/T_s. But, after applying these equations, it is found that difference between maximum and minimum values of the tension ratio is about 15%, which is small as compared to estimating loads in many actual conveyor belt systems. So, in practice, the Euler's formula is acceptable in engineering application.

Kim et al. [16] investigated theoretically the belt behavior to determine the effect of belt velocity on normal and tangential belt forces and centrifugal tension. Kim et al. [17] studied the friction characteristics between an abrasive belt and a driver and driven pulley. Normal and tangential forces have been measured using two different belt pulley interface force transducers. These forces were found to change almost linearly rather than in an exponential manner as predicted by classical Euler's equation. The theoretical and experimental data are closely matching. Virabov

[18] has studied effect of centrifugal forces on behavior of belt drives and depends on the ratio between the elasticity of shafts and belt.

Zhang and Zu [19] has solved the coupled non-linear equations of motion of serpentine belt drive systems using the direct multiple scales method. It is shown that the direct multiple scales method yields better results for the system than the ordinary discretization multiple scales method. Kwon and Ih [20] proposed method for obtaining the physical characteristics of the transverse vibrational power flow through moving rubber belts and shown that the vibrational power of the two belt-spans flows into the tensioner. It is shown that the energy flow agrees reasonably well with the predicted results. Pellicano et al. [21], investigated the effect of pulley eccentricity on the vibration of a power transmission belt and a theoretical model is developed for validation and identification purposes. Comparisons between analytical solution and experimental data allow the identification of the unknown parameters of the analytical model.

Iwatsubo et al. [22] presented a method for analyzing the dynamic characteristics of driving systems consisting of multiple belts and pulleys. Firstly, an algorithm that derives the linear equations of motion for arbitrary multi-coupled belt systems is given. Complicated belt systems consisting of multiple belts and pulleys are regarded as combinations of simple belt systems consisting of a single belt and several pulleys. Therefore, superposing the equations of motion for the simple belt systems can derive the equations of motion for the belt systems and responses of the arbitrary multi-coupled belt systems can be calculated. Moon and Wickert [23] performed laboratory measurements to identify a particular source of vibration excitation for v-belts that is attributed to lateral misalignment of the sheaves. Zhang and Zu [24] performed the modal analysis of linear prototypical serpentine belt drive systems in this study. The response of serpentine belt drive systems to arbitrary excitations is obtained as a superposition of orthogonal eigenfunctions. Rim and Kim [25] introduced a method of identifying both static and dynamic components of belt tension under operating conditions in this work, which contain all the information on the state of power transmission. The static component corresponds to the steady state power transmission while non-circularity or eccentricity of the pulley system surface irregularity of belt and pulley, dynamic loading, etc. are responsible for the dynamic component. Frequency characteristics of transient vibrations of the belt caused by an impact on it are analyzed and related to the static and dynamic components of the tension. An appropriate parameter representing the overall quality of the belt driving systems is proposed. Kim and Lee [26] proposed a mathematical model for a belt-driven system to analyze vibration characteristics of driving units having belts, and free and forced vibration analyses are carried out. The mathematical model for a belt-driven system includes belts, pulleys, spindle and bearings. The material properties of each belt and the equivalent stiffnesses supported by pulleys, bearings and a spindle are calculated through experiments. By using Hamilton's principle, four non-linear governing equations and 12 non-linear boundary conditions are derived. To linearize and discretize the non-linear governing equations and boundary conditions, the perturbation and Galerkin methods are used. Also, the free vibration analyses for various parameters of a belt-driven system are made, including the tension of a belt, the length of a belt, the material properties of belts, the belt velocity and the pulley mass. Forced vibration analyses of the system are performed, and the dynamic responses for the main parameters are analyzed for a belt-driven system.

2. Problem formulation

Modak [11] suggested three approaches for studying mechanism of torque transmission from rim to the shaft through the arms of the pulley [11]:

1. Equal distribution of load zone by the arm based on highly simplified assumption.
2. Equilibrium of rim portion.
3. Qualitative analysis of a suggestion for an approach by FEM.

2.1. Equal distribution of load zone by the arm

This is first of the three above-stated approaches for analyzing the mechanism of torque transmission of a driven pulley of a belt drive. This approach is based on two assumptions:

1. Rim is thin, almost a lamina.
2. Number of arms present in the load zone takes charge of the load zone angle equally as they appear in the load zone.

Driven pulley of a belt drive rotating clockwise is as shown in Fig. 1. The arms of the pulley are designated as OA, OB, OC, OD, OE and OF. Arm OA is assumed to coincide with radial line O1 at any instant of time $t = t_1$. At this instant, four arms OA, OB, OC and OD are in the load zone. During further rotation, when OD coincides with O2, at an instant $t = t_2$, only three arms OA, OB and OC will remain in the load zone. Hence during the time duration $(t_2 - t_1)$, four arms are in the load zone. During further rotation of the pulley, arm OF coincides with O1, at an instant $t = t_3$. Hence during the time $(t_3 - t_2)$, three arms are in the load zone. Hence the arm, during its traversal in the load zone is subjected to varying load as shown in Fig. 2. The computer simulation of dynamic and vibration response of flat belt drive pulley based on this approach was reported [12]. In this work, a cursory idea of stress under vibration is achieved and response of an equivalent spring, mass and damper system is achieved. Comparing the natural frequencies of the model with other methods checks accuracy of the model.

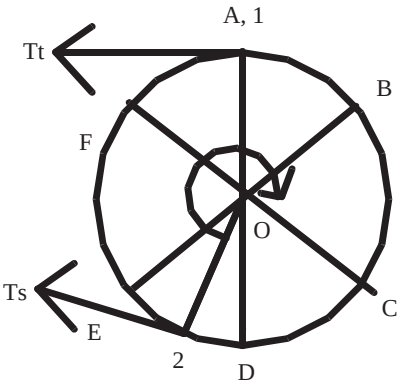

Fig. 1. Driven pulley of a belt drive.

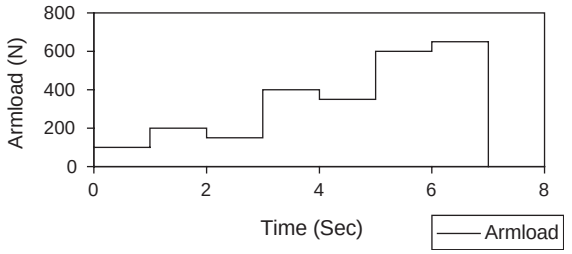

Fig. 2. Variation of armload as a function of time.

2.2. Equilibrium of rim

In this approach, equilibrium of the portion of the rim under the angle of lap or in the load zone is considered. But the rim is assumed thin, almost like a lamina. The second assumptions in the first approach i.e., the number of arms present in the load zone takes charge of the load zone angle equally as they appear in the load zone, is removed. This equilibrium equation leads to establishing frictional force produced by the belt on the rim, balanced by the reaction of the arm under consideration at the rim–arm interface. This approach has two possible solutions each one leading to an equation of equilibrium of the portion of the rim. These equations have solution but are not mathematically solvable in the closed form. Hence these equations can be solved on a computer by iteration. A generalized algorithm can be suggested for finding the armload variation and stresses in the arm.

The outer surface of the rim is in contact with the belt and because of the friction between them, motion of the pulley occur as shown in Fig. 1. Frictional force exerted by the belt element on portion of the rim, subtending an angle $\delta\phi$, is as shown in Fig. 3. This elemental frictional force is given by

$$\delta F_f = \mu T \delta\phi. \tag{1}$$

Frictional force per unit length of the arc of contact can be established as

$$\begin{aligned} \delta F_f / R\delta\phi &= \mu T \delta\phi / R\delta\phi \\ &= \mu T / R. \end{aligned} \tag{2}$$

By Euler's equation, tension in the belt at any angle ϕ is given by, $T = T_s e^{\mu\phi}$, substituting in Eq. (2), we get

$$\delta F_f / R\delta\phi = (\mu/R) T_s e^{\mu\phi}. \tag{3}$$

This frictional force is balanced by force produced by arm OA at A.

Fig. 4 shows portion of the rim, subtending angle 104, in which arm OA is present during the time instant $(t_3 - t_1)$. This angle is divided into three parts subtending angle $\delta\phi_1$, $\delta\phi_2$, $\delta\phi_3$ from line 01 and arm OA is assumed to be present in this load zone. The frictional force, δF_{f1}, corresponding to angle 102, is assumed to act at an angle $\delta\phi_1/2$ from line 01. The frictional force, δF_{f2}, corresponding to angle 203, is assumed to act at an angle $(\delta\phi_1 + \delta\phi_2/2)$ from line 01 and so

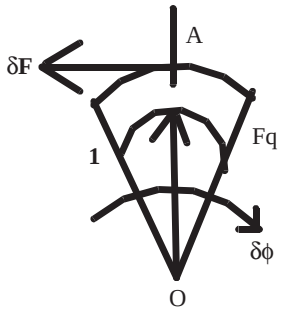

Fig. 3. Portion of the rim-subtending angle $\delta\phi$, subjected to frictional force δF_f due to belt–pulley interaction.

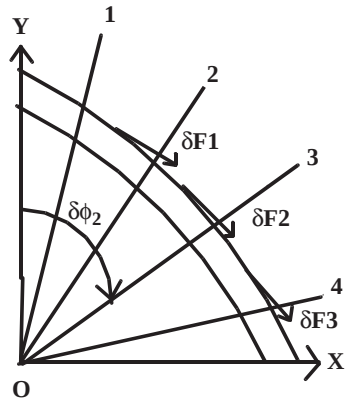

Fig. 4. Portion of rim under the action of system of forces.

on. The other force acting on the rim is produced by arm OA at A, neglecting the force produced by the remaining portion of the rim on the portion under consideration. Hence the portion of the rim under consideration is assumed to be under equilibrium by two forces, viz.,

1. Resultant of all δF_f's.
2. Reaction of the arm OA at A on the rim.

Then, for this configuration, the reaction of the force produced by OA at A on the rim is the load on the arm. For this consideration to be satisfied there are two possibilities:

1. The resultant of all δF_f's is passing through OA may be oblique to OA.
2. The resultant of all δF_f's is not passing through OA. In this case OA may be required to supply certain unbalanced couple.

Then, for this configuration, as shown in Fig. 5 the reaction of the force produced by OA at A on the rim is the load on the arm, F_a.

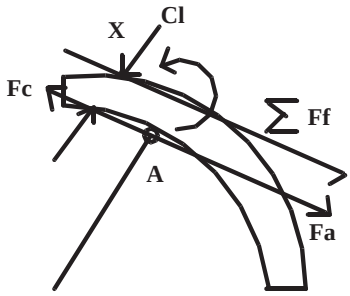

Fig. 5. Free body diagram of the rim (Singru and Modak).

As shown in Fig. 5, if the resultant of all the frictional forces is passing through A, i.e., first possibility, the $X = 0$ and there is no unbalanced couple. But if the resultant of all the frictional forces is not passing through A, i.e., second possibility, then there is some distance X from A at which the ΣF_f will pass. This leads to presence of unbalanced couple at the rim. The presence of this unbalanced couple can be shown by applying two equal and opposite forces of the magnitude ΣF_f, passing through A, denoted by F_a and F_c. As shown in Fig. 5, the force F_c and ΣF_f creates the unbalanced couple and F_a is the armload. (Neglecting the force exerted by the remaining portion of the rim on the portion of lamina under consideration.) The armload F_a is then resolved into two components F_{tan} and F_{nor}. F_{tan} is perpendicular to the arm OA and F_{nor} is passing axially through A inward. Considering the centrifugal force on the arm and the rim due to rotation, acting radially outwards, F_{ca} and F_{cr}. The unbalanced couple at the rim is balanced by equal and opposite couple at the arm. This couple is given by

$$C_{unbal} = F_{tan}X. \tag{4}$$

Equivalent force system acting on the arm, balancing the unbalanced couple at the rim is given by two equal and opposite forces F_{couple}, one acting at the rim end of the arm and other acting at the hub end of the arm, separated by distance l, the length of arm. F_{couple} is given by

$$F_{couple} = C_{unbal}/L. \tag{5}$$

2.3. Qualitative analysis of a suggestion for an approach by finite element method

Modak [11] suggested finite element analysis of the complete pulley subjected to load variation found using two approaches. A three-dimensional model of the complete pulley should be created, discritized with suitable elements. Load variation found using two approaches should be applied with given boundary conditions and dynamic response of the arms should be found. Three-dimensional beam element and brick element will be considered to analyze the problem. This work is in advanced stage and will be published soon [36].

3. Analysis of rim

In this section the equilibrium of the rim is considered as per second approach discussed in Section 2.2. The rim is to be iteratively analyzed to find the forces acting on the arm. The angle of lap is divided into equal sectors of "turn" degrees and this sector "turn" is divided into "*d*" number of divisions. As an example of six-arm pulley shown in "Fig. 1", variation of armload as the arm sweeps the active load zone of 190° can be found by dividing the load zone in eight parts. Arm under consideration is arm A. The armload is different at every instant; the angle of lap is divided into eight different sectors. These divisions are based on the case of whether four arms are in the load zone or three arms are in the load zone. Here the eight cases are for arm in following instants. Depending on these conditions variation of armload is calculated as follows. Figs. 6–13 shows only the arms which are in the load zone. Equations so derived in these subsequent cases are iterative equations presented in Table 1. An iterative algorithm in C like syntax for finding the armload is stated in Appendix B. Some repetitive steps are not stated in the algorithm.

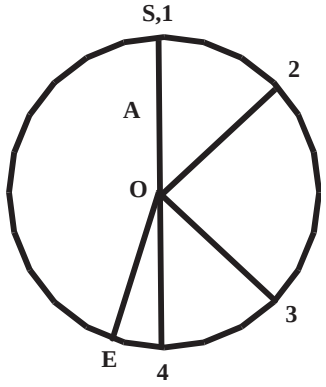

Fig. 6. The instantaneous position of arm A at the instant when it is entering the load zone.

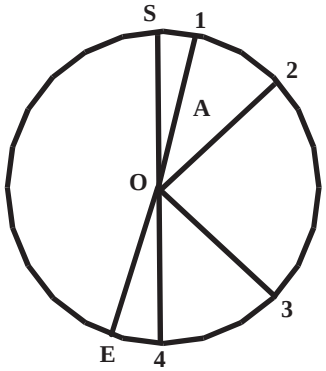

Fig. 7. The instantaneous position of arm A at the instant when it is in sector of 0–10°.

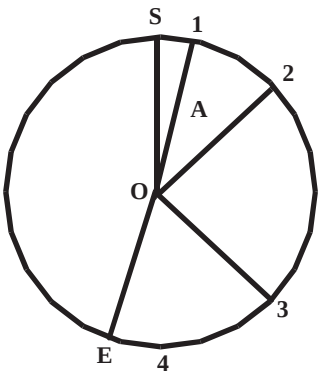

Fig. 8. The instantaneous position of arm A at the instant when it is in sector of 10–60°.

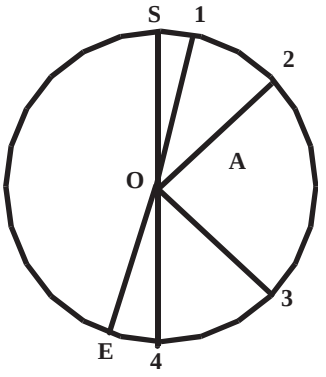

Fig. 9. The instantaneous position of arm A at the instant when it is in sector of 60–70°.

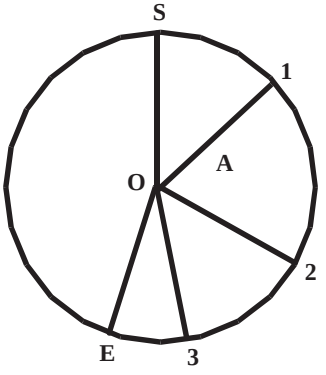

Fig. 10. The instantaneous position of arm A at the instant when it is in sector of 70–120°.

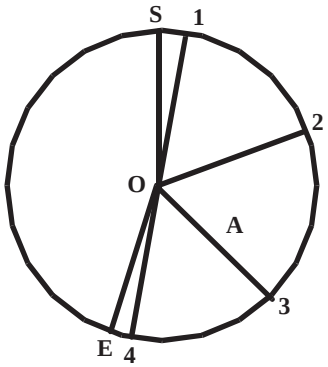

Fig. 11. The instantaneous position of arm A at the instant when in sector of 120–130°.

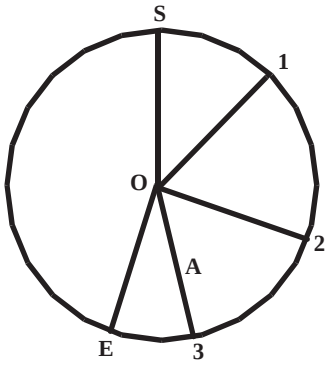

Fig. 12. The instantaneous position of arm A at the instant when it is in sector of 130–180°.

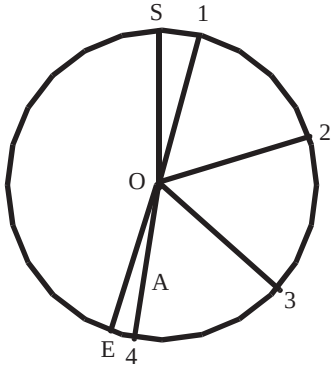

Fig. 13. The instantaneous position of arm A at the instant when it is in sector of 180–190°.

Table 1
Iterative equations of elemental frictional forces in different load zones

S. no.	Position of arms	Iterative equations	Equation no.
1.	At the entry of load zone	None	
2.	Between 0° and 10°	$\delta f_{fi} = \mu T_2 e^{\mu(sum+\delta\phi_i/2)}\delta\phi_i$	6
		$sum = 0;\ sum = sum + (\delta\phi - \phi/d),$	7
		$\phi = turn(\pi/180)$	8
3.	Between 10° and 60°	$\delta f_{fi1} = \mu T_2 e^{\mu(sum+\delta\phi_{i1}/2)}\delta\phi_{i1}$	9
		$\delta f_{fi2} = \mu T_2 e^{\mu(\phi+sum+\delta\phi_{i2}/2)}\delta\phi_{i2}$	10
		$sum = 0; sum = sum + (\delta\phi - \phi/4)$	11
		$\phi = turn(\pi/180)$	12
4.	Between 60° and 70°	$\delta f_{fi} = \mu T_2 e^{\mu(\phi+sum+\delta\phi_i/^2)}\delta\phi_i$	13
		$sum = 0; sum = sum + (\delta\phi - \phi/4)$	14
		$\phi = (turn - 60)(\pi/180)$	15
5.	Between 70° and 120°	$\delta f_{fi} = \mu T_2 e^{\mu((turn\ \pi/180)+sum+\delta\phi_i/2)}\delta\phi_i$	16
		$sum = 0; sum = sum + (\delta\phi - \phi/4)$	17
		$\phi = (turn - 60)(\pi/180)$	18
6.	Between 120° and 130°	$\delta f_{fi} = \mu T_2 e^{\mu((turn\ \pi/180)+sum+\delta\phi_i/2)}\delta\phi_i$	19
		$sum = 0; sum = sum + (\delta\phi - \phi/4)$	20
		$\phi = (turn - 60)(\pi/180)$	21
7.	Between 130° and 180°	$\delta f_{fi} = \mu T_2 e^{\mu((turn\ \pi/180)+sum+\delta\phi_i/2)}\delta\phi_i$	22
		$sum = 0; sum = sum + (\delta\phi - \phi/4)$	23
		$\phi = (turn - 60)(\pi/180)$	24
8.	Between 180° and 190°	$\delta f_{fi1} = \mu T_2 e^{\mu(\phi+sum+\delta\phi_i 1/2)}\delta\phi_{i1}$	25
		$\delta f_{fi2} = \mu T_2 e^{\mu((turn\ \pi/180)+sum+\delta\phi_i 2/2)}\delta\phi_{i2}$	26
		$sum = 0; sum = sum + (\delta\phi - \phi/4)$	27
		$\phi = (turn - 60)(\pi/180)$	28

3.1. Case 1

As shown in Fig. 6 when the arm A is just on the verge of entering the load zone, the load acting on the arm under consideration is zero. The load corresponding to sector SO2 acts on arm O2, the load corresponding to sector 2O3 acts on arm O3 and loads corresponding to sector 3OE acts on arm O4. During this instant four arms in the load zone.

3.2. Case 2

This is the case of instant when the arm A has turned through an angle less than (lap-180) i.e., 10° as shown in Fig. 7 in this case. Four arms are present in the load zone and load is distributed among all the arms. The load of sector SO1 acts on arm O1 or A, load of sector 1O2 acts on arm O2, load of sector 2O3 acts on arm O3, load of sector 3OE acts on arm O4. Load on arm A increases as it turns from 0° to 10°. The frictional force is given in Table 1.

3.3. Case 3

This is the case of the instant when the arm A has turned through an angle more than or equal to (lap-180) i.e., 10° but less than 60° as shown in Fig. 8. At this instant the arm O4 goes out of the

load zone and there are three arms in the load zone. Load of sector SO2 act on arm O1, load of sector 2O3 act on O2, load of sector 3OE act on O3. The load on arm OA gradually increases as it turns from 10° to 60°. The frictional force is given in Table 1.

3.4. Case 4

This is the case of an instant when the arm A has turned through an angle greater than 60° and less than 70° as shown in Fig. 9. At this instant the arm under consideration (arm A) becomes the second arm in the load zone, as a new arm enters into the load zone. Again it becomes a case of four arms. Load of sector SO1 act on arm O1, load of sector 1O2 act on arm A, load of sector 2O3 act on arm O3, load of sector 3OE act on arm O4. Load on the arm OA decreases in this zone. The frictional force is given in Table 1.

3.5. Case 5

This is the case of the instant when the arm A has turned through an angle greater than 70° and less than 120° as shown in Fig. 10. There are again three arms in the load zone. The load is taken by the first arm O1 corresponding to sector SO2, load of sector 2O3 is taken by arm O3. During this period the load on arm OA will go on increasing as the load sector increases from 70° to 120°. The frictional force is given in Table 1.

3.6. Case 6

This is the case of the instant when the arm A has turned through an angle greater than 120° and less than 130° as shown in Fig. 11. There are four arms in the load zone due to entry of new arm in it. The arm under consideration is now the third arm in the load zone. Load of sector SO1 is taken by arm O1; load of sector 3O4 is taken by arm O4, load of sector 1O2 is taken by arm O2, and load of sector 2O3 is taken by arm OA. There is increase in load in this zone. The frictional force is given in Table 1.

3.7. Case 7

This is the case of the instant when the arm A has turned through an angle greater than 130° and less than 180° as shown in Fig. 12. There are three arms in the load zone now. Maximum load is taken by arm O1 corresponding to sector SO2, load of the sector 2O3 is taken by arm O2, and load of the sector 3OE is taken by arm A. The load on arm A will increase suddenly after angle of turn exceeds 130° and then the load decreases. The frictional force is given in Table 1.

3.8. Case 8

This is the case of the instant when the arm has turned through an angle greater than 180° and less than or equal to 190° as shown in Fig. 13. There are four arms in the load zone. The arm A now becomes the fourth arm. The load of sector SO1 is taken by arm O1, the load of sector 1O2 is taken by arm O2, the load of sector 2O3 act on arm O3, the load of sector 3OE act on arm A

(i.e., arm O4). Load increases suddenly when angle becomes more than 180° and then decrease onto 190°. The frictional force is given in Table 1.

4. Case study

This paper is in continuation of paper published by Singru and Modak [12]. In that paper analytical results were applied to a case study and the cursory idea of stress under vibration is calculated using first approach [11,12]. This work is continuation of the previous work using second approach [11,12]. This approach gives us the tangential and normal components of armload, the unbalanced couple present at the arm–rim interface and stress under vibration. A comparison of the results obtained by these two approaches is done. By this simulation study it can be concluded that belt flutter occurs due to presence of this unbalanced couple present at the arm–rim interface.

4.1. Design of belt drive

The design of belt drive was performed using software CADOM [27–30].

Input power = 21 kW, speed of driving pulley = 750 r.p.m, speed of driven pulley = 250 r.p.m. The software gave the following design specification of the flat belt drive and pulley. Specification of driven pulley—material ISC 30, diameter = 1247 mm, diameter of shaft = 63 mm, diameter of hub = 172 mm, length of hub = 94.5 mm, number of arms = 6, cross-section of the arm is elliptical with a taper of 1 in 40. Arm specifications are—length of major axis at the hub = 90 mm, length of minor axis at the hub = 45 mm, width of the rim = 142 mm, thickness of the rim = 16.24 mm, crown of the rim = 1.42 mm, angle of lap = 3.33 rad = 190°, length of the arm = 529.28 mm, volume of the arm = 0.0011073037229 m^3, mass density of material = 7.2×10^3 kg/m^3, distance of centroid from the axis of rotation = 0.3178 m, modulus of elasticity = 9.1×10^4 MPa, tension on slack side = 1771.77 N, tension on tight side = 4978.6678 N, average moment of inertia of the cross section of arm = 1.005×10^{-6} m^4.

4.2. Computer simulation

For the particular driven pulley, designed in Section 4.1, the necessary portion of the rim is to be ascertained by iterative process of getting resultant of δf_f's, which is armload and unbalanced couple. Computer simulation for the system is performed, to get the variation of the tangential and normal components of armload, the unbalanced couple present at the arm–rim interface and stress under vibration.

The computer simulation of the above system is undertaken for the pulley design stated above. Force equilibrium for the arm, shown in Fig. 4, is considered. The variable "turn", the angle considered for iteration taken at a time out of total angle of lap, "lap", on which the sum of elementary frictional forces are considered, is varied from 1 to 20 with increment of 1. Number of divisions of each angle of "turn", is varied from 1 to 20. This variation is done in order to ascertain the rim by iteration. This process gave us different data files. Graphs for tangential, normal component of armload, and unbalanced couple are created for angle of iteration, "turn"

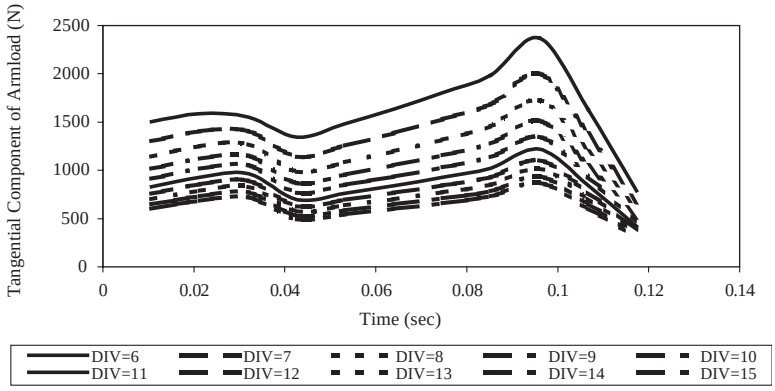

Fig. 14. Tangential component of armload (angle = 6° and div = 6–15).

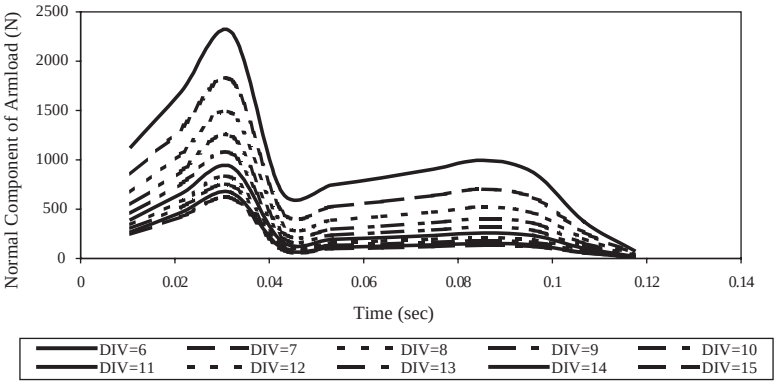

Fig. 15. Normal component of armload (angle = 6° and div = 6–15).

varying from 6° to 17° and each angle is divided into number of divisions varying from 6 to 15. The representative graphs are as shown in Figs. 14–16, for angle 6° and Figs. 17–19 for angle 16°, the number of divisions of this angle are varied from 6 to 15. The other graphs for angle "turn" varying from 7° to 17°, are drawn by the author but not attached here due to space constraints.

5. Equation of motion

The arm of the driven pulley of flat belt drive is considered as cantilever beam subjected to tangential load, normal load and centrifugal load due to pulley rim and arm. From Figs. 15 and 18 it is clear that the normal component of armload is small after 60° i.e., after time instant of 0.04 s. However the values of tangential component of armload and force due to unbalanced couple, F_{couple} is large in this zone. Hence we are neglecting normal component of armload as well as centrifugal load due to pulley rim and arm itself. Considering $F(t) = F_{tan} + F_{couple}$ as total load

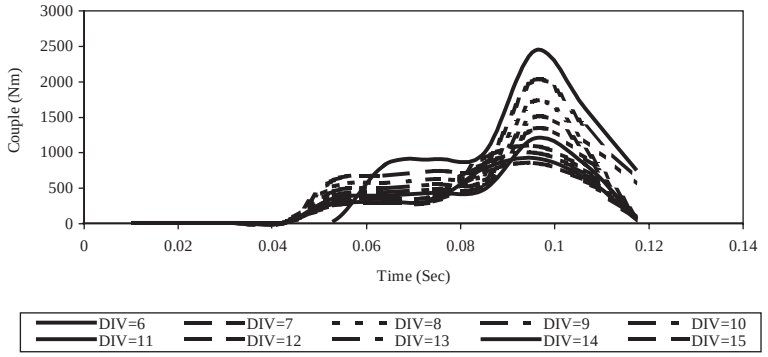

Fig. 16. Unbalanced couple acting at arm–rim interface (angle = 6° and div = 6–15).

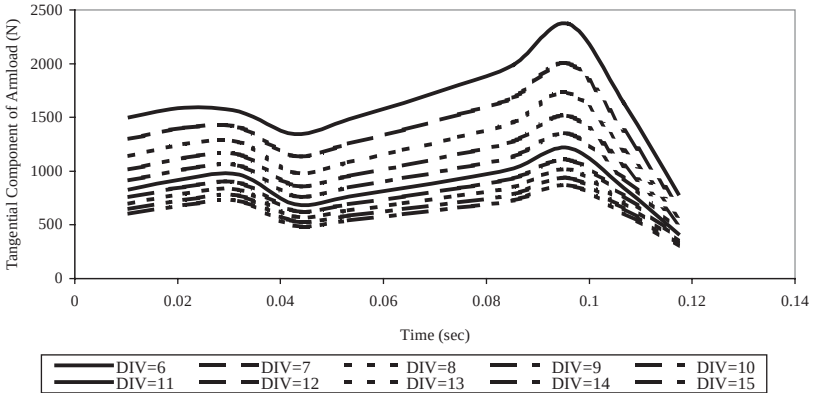

Fig. 17. Tangential component of armload (angle = 16° and div = 6–15).

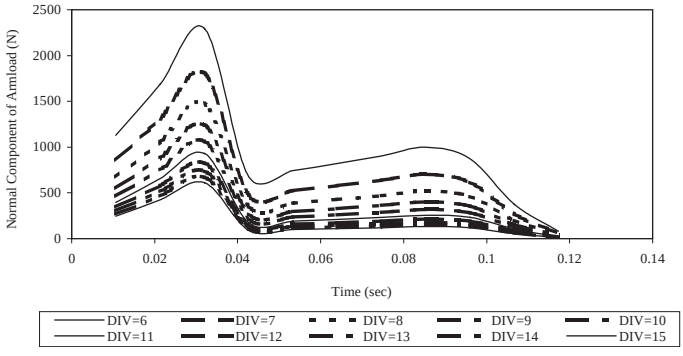

Fig. 18. Normal component of armload (angle = 16° and div = 6–15).

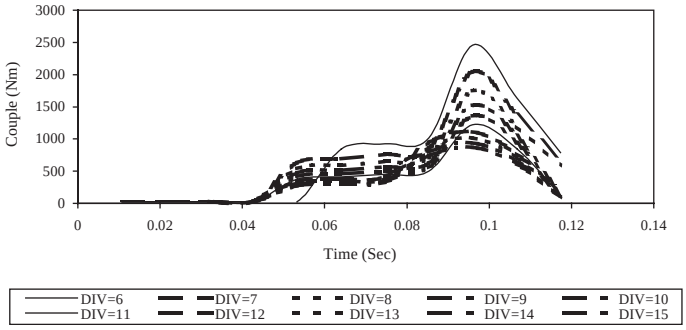

Fig. 19. Unbalanced couple acting at arm–rim interface (angle = 16° and div = 6–15).

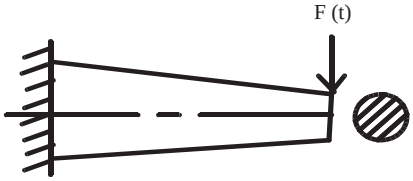

Fig. 20. Arm of a belt drive pulley.

acting on the arm. The equation of motion of the arm is found by making some more assumptions:

1. Arm is considered as cantilever beam fixed at the hub as shown in Fig. 20.
2. Mass of the arm is assumed to be concentrated at the tip i.e., at the rim of the pulley.
3. Damping present in the arm, called structural damping, is considered in terms of equivalent viscous damping.
4. Stiffness of cantilever at the tip is considered as equivalent spring stiffness.

5.1. Equivalent mass

The equivalent mass of the arm is given by [31]

$$M_{eq} = (mr_g)/L. \tag{29}$$

Here the mass of the rotating arm is transferred to its tip by Eq. (29).

5.2. Equivalent spring stiffness

For a cantilever beam subjected to a load at the tip [32], the stiffness is given by

$$K_{eq} = 3EI/L^3. \tag{30}$$

5.3. Equivalent viscous damping

In this case the structural damping inside the material of the beam can be modelled as equivalent viscous damping [32,33]. Structural-damping information is well compiled by Lazen [34]. But all the

values of loss coefficients, with which we can find equivalent viscous damping, are valid for harmonic excitation. Our excitation is different from harmonic excitation; hence, it is difficult to calculate the exact value of structural damping. Hence only equivalent viscous damping is assumed.

The equivalent viscous damping coefficient is hence given by

$$C_{eq} = M_{eq} 2\xi\omega_n, \tag{31}$$

where

$$\omega_n = \sqrt{(K_{eq}/M_{eq})}. \tag{32}$$

We are not considering damping in our analysis here because in the analysis using first approach we have considered free vibrations. So we are assuming $\xi = 0$ and proceed for finding equation of motion:

5.4. Equation of armload

The equivalent spring, mass and damper system as shown in Fig. 21, has following governing differential equation of motion:

$$M_{eq}\mathrm{d}^2x/\mathrm{d}t^2 + C_{eq}\mathrm{d}x/\mathrm{d}t + K_{eq}x = F(t). \tag{33}$$

This armload $F(t)$, using Eq. (5) is $f = F_{tan} + F_{couple}$. The nature of f is such that it can be considered as a continuously varying forcing function. A continuous forcing function can be analyzed by the same methods as a sequence of impacts if it is first converted into such a sequence [31]. The continuous force–time curve is broken into increments with respect to time and each increment is an impulse of the form $f\,\mathrm{d}t_i$ as shown in Fig. 22.

As damping is not considered here $C_{eq} = 0$, then system equation becomes

$$M_{eq}\mathrm{d}^2x/\mathrm{d}t^2 + K_{eq}x = F(t). \tag{34}$$

The equation of motion for a simple spring mass system subjected to impulse of very short duration $f\,\mathrm{d}t_i =$ impulse is given by [31]

$$x = \Sigma((\text{impulse})_i/(M_{eq}\omega))\sin\omega(t - t_i). \tag{35}$$

For a continuous sequence of impulses, the summation sign is replaced by integration,

$$x = \int_0^t ((f\,\mathrm{d}t_i)/(M_{eq}\omega_n))\sin\omega_n(t - t_i). \tag{36}$$

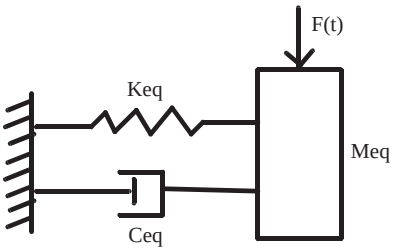

Fig. 21. Equivalent spring, mass and damper system.

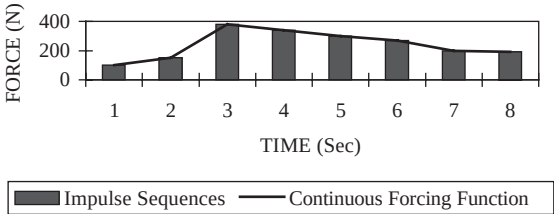

Fig. 22. The continuous force–time curve broken into increments with respect to time and each increment is an impulse of the form $f\,\mathrm{d}t_i$.

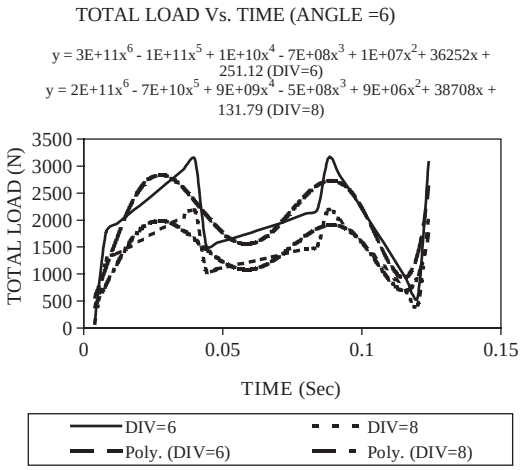

Fig. 23. Force acting on the arm, f, for angle $= 6^\circ$ and div $= 6$ and 8, with its polynomial best-fit curve (a representative case).

Hence,

$$x = \int_0^t (f/M_{eq}\omega_n)(\sin\omega_n t\cos\omega_n t_i - \sin\omega_n t_i\cos\omega_n t)\,\mathrm{d}t_i. \tag{37}$$

We hold natural frequency of system to be constant; we get amplitude of system as

$$x = (\sin\omega_n t/M_{eq}\omega_n)\int_0^t (f\cos\omega_n t_i)\,\mathrm{d}t_i - (\cos\omega_n t/M_{eq}\omega_n)\int_0^t (f\sin\omega_n t_i)\,\mathrm{d}t_i. \tag{38}$$

The nature of forcing function f is as shown in Fig. 23, a representative case is only considered here. There are two methodologies of solving the equation of motion:

1. Considering a best-fit polynomial for the force-time variation.
2. Numerically computing the value of f at every instant and evaluate above equation numerically at every instant of time. But the accuracy of these results depends on value of $\mathrm{d}t_i$. During the simulation using this method it is found, if $\mathrm{d}t_i = 0.0067$ s, the deflection comes in the range of 0.8–0.9 m. For the value of $\mathrm{d}t_i = 0.0000067$ s, the deflection comes in the range of 3–4 mm which is realistic.

Hence we are considering the first approach here i.e., a best-fit polynomial of sixth degree for our analysis. As shown in Fig. 23, it closely approximates the complete curve for two representative and different sets of values of f found during the process of iteration (for angle = 6° and div = 6 and 8).

Hence equation of f is assumed as

$$f = a_0 + a_1 t_i + a_2 t_i^2 + a_3 t_i^3 + a_4 t_i^4 + a_5 t_i^5 + a_6 t_i^6. \tag{39}$$

Substituting the equation of f in above equation of x, we get

$$x = (\sin \omega_n t / M_{eq} \omega_n) \int_0^t ((a_0 + a_1 t_i + a_2 t_i^2 + a_3 t_i^3 + a_4 t_i^4 + a_5 t_i^5 + a_6 t_i^6) \cos \omega_n t_i)\, \mathrm{d}t_i$$
$$- (\cos \omega_n t / M_{eq} \omega_n) \int_0^t ((a_0 + a_1 t_i + a_2 t_i^2 + a_3 t_i^3 + a_4 t_i^4 + a_5 t_i^5 + a_6 t_i^6) \sin \omega_n t_i)\, \mathrm{d}t_i.$$

Performing the integration and substituting the limits, we get, the deflection of arm, as

$$\begin{aligned} x = {} & (\sin^2 \omega_n t / M_{eq} \omega_n^2)\,(K_1 + K_2 t + K_3 t^2 + K_4 t^3 + K_5 t^4 + K_6 t^5 + K_7 t^6) \\ & - (\cos^2 \omega_n t / M_{eq} \omega_n^2)(K_{14} + K_{15} t + K_{16} t^2 + K_{17} t^3 + K_{18} t^4 + K_{19} t^5 + K_{20} t^6) \\ & + (\sin \omega_n t \cos \omega_n t / M_{eq} \omega_n^3)((K_8 - K_{21}) + (K_9 - K_{22}) t + (K_{10} - K_{23}) t^2 + (K_{11} - K_{24}) t^3 \\ & + (K_{12} - K_{25}) t^4 + (K_{13} - K_{26}) t^5) + K_{14} / (M_{eq} \omega_n^2). \end{aligned} \tag{40}$$

The equations for K_1 to K_{26} are given in Appendix A.

5.5. Stress under vibration

The stress under vibration is calculated in the same manner as that of first approach [12]. As the arm is subjected to varying load, it is subjected to stress under vibration. Equivalent dynamic load, F_{dy} required to calculate the stress is given by

$$F_{dy} = 3EIx / L^3. \tag{41}$$

Stress is thus given by

$$\sigma_{arm} = F_{dy} L / Z. \tag{42}$$

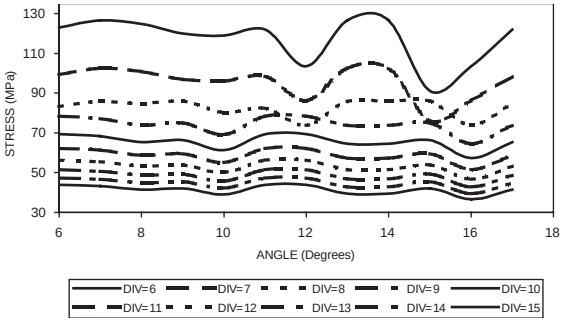

Fig. 24. Maximum stress under vibration for angle of iteration, "turn", under consideration in the range 6°–17° and number of divisions of this angle in the range of 6–15.

The stress in arm is found from each graph and a plot between stresses in arm as a function of angle for different number of divisions is as shown in Fig. 24.

6. Presence of unbalanced couple and phenomenon of belt flutter

As shown in Fig. 5, there is some unbalanced couple at the rim. In problem formulation, we have discussed that the reaction couple provided by the arm is balancing this unbalanced couple. There is a common phenomenon in the flat belt drive i.e., belt flutter. During the rotation of the pulley in the active load zone, it is observed that there is a belt flutter i.e., the belt leaves the contact momentarily and again the contact with the pulley is established. During our observation in our case study, it is found that belt flutter is observed at a definite angle from the entry position of belt in the load zone. For a 190° angle of lap pulley, it is observed that the belt flutter is occurring in the last 1/3rd portion of lap angle. The reasons given by field experts are loosening of belt and change in contact surface friction properties. But even if the belt is properly tightened and designed friction properties are present, belt flutter occurs in armed pulleys. The reason we are putting for belt flutter is as follows. The value of unbalanced couple is zero during initial portion of angle of lap i.e., for $\varphi = 190°$, $C_{unbal} = 0$ upto $\varphi = 60$–$65°$. Then C_{unbal} starts increasing and it is observed that its value is maximum at $\varphi = 135$–$150°$. After the maximum the next value of C_{unbal} reduces drastically, almost near to zero. This means that when C_{unbal} is at maximum, the arm A is not in a position to provide sufficient equal and opposite reaction couple to the unbalanced couple at the rim. Not only arm but also there are two more mechanisms, which are able to provide reaction couple viz. reaction couple provided by the portion of belt in contact with the portion of lamina under consideration as shown in Fig. 25 and remaining portion of lamina shown in Fig. 26.

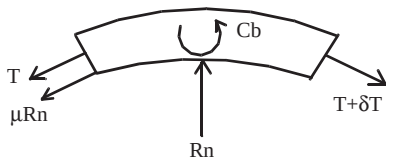

Fig. 25. Reaction couple provided by the portion of belt in contact with the portion of lamina under consideration.

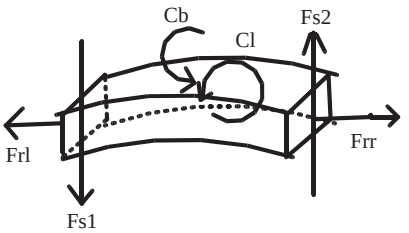

Fig. 26. Reaction couple provided by the remaining portion of lamina on the lamina under consideration.

6.1. Reaction couple produced due to portion of belt in contact with the lamina on lamina under consideration

Reaction couple provided by the portion of belt in contact with the portion of lamina under consideration as shown in Fig. 25. The resultant of forces T and $T + \delta T$ is passing through nearly the center of belt thickness wise. This resultant force as well as the frictional force μRn provides the counterclockwise reaction couple, C_b to the rim to balance the unbalanced couple produced in the rim.

6.2. Reaction couple provided by remaining portion of the lamina on lamina under consideration

The remaining portion of the lamina exerts tensile forces F_{rl} and F_{rr} and shear force F_{s1} and F_{s2} on the lamina under consideration as shown in Fig. 26. This system of forces provides the reaction couple C_l on the rim.

6.3. Explanation of belt flutter

The equilibrium of portion of lamina when considered leads to the fact that resultant of frictional force is not passing through A and there is presence of certain couple which is balanced by two systems of forces as per Sections 6.1 and 6.2. During initial rotation of the pulley, this couple is small and might be getting balanced by reaction forces provided by belt and remaining portion of lamina. But as this couple C_{unbal} increases, after some angle of rotation and it is maximum at certain angle of rotation in the angle of lap, the C_b and C_l is not sufficient to balance it. This is leading to separation of belt from the pulley momentarily causing belt flutter commonly occurring in belt drives.

7. Results and discussion

The result of computer simulation of system discussed in Section 4.2 and equation of motion discussed in Section 5 can be summarized using Eqs. (40) and (42). Results of this approach are compared with that of first approach in Table 2 [12].

1. From Table 2 it is clear that the second approach results are more refined than the first approach results even though the results are not converging. The results of second approach in

Table 2
Comparison table of results by first and second approach

S. no.	Approach	Deflection of arm (mm)	Stress under vibration (MPa)
1.	First approach [12]	4.18	57.055
2.	Second approach (with turn = 6–17° and no. of division = 6–15. The solution is not converging. So a range of values is given)	4.23–3.45	59.12–36.094

the range of turn = 6–17° and d = 6–15, are showing that stress under vibration comes out to be lower than the first approach. Thus this approach is more refined.

2. In the case study, graph between maximum stress under vibration for angle of iteration "turn" taken at a time out of angle of lap "lap", in the range of 6–17° and number of divisions of this angle are made to find the frictional force acting on that portion of the rim, in the range of 6–15, shown in Fig. 24.
3. The minimum value of stress under vibration is occurring at an angle of 16° when this angle is divided into no. of divisions varying from 8 to 15. This simply means that the maximum stress under vibration is minimum for the angle of 16° irrespective of no. of divisions. Stress induced for angle = 16° and no. of divisions = 10–15 is in the range of 57.22–36.094 MPa. For pulley material ISC 30, ultimate tensile strength, S_{ut} = 527 MPa, Factor of safety = 8. Design stress S_d = 65.9 MPa. This means that for no. of divisions = 10–15, the maximum stress developed is less than the design stress. So there is over design.
4. A reasonable angle of 6–17° and no. of divisions 6–15 is sufficient to analyze the problem.
5. The values of maximum stress under vibration for angle = 16° and div = 10–15 are less than the values obtained in the first approach, equal to 57.055 MPa. [12] This shows that second approximation is more refined than the previous approach, even though the solution is not converging mathematically. Hence we could conclude that by this approach, we get cursory idea of nature of variation of stress under vibration.
6. When number of divisions is increased from 6 to 15, for all maximum values of angle of iteration "turn" for which the unbalanced couple is zero varies in the range of 51–81°. This means resultant frictional force is passing through the tip of the arm unto this zone. But for the angle of iteration, taken at a time, for calculating frictional force equal to 16°, the zero unbalanced couple angle is 64° irrespective of no. of divisions of angle of iteration.
7. The presence of unbalanced couple is a phenomenon needs to be analyzed in details. This unbalanced couple shows its presence when the arm A, under consideration, is at an angle of 60–70° depending on angle of iteration and number of divisions of this angle. This sudden presence of unbalanced couple is because of presence of fourth arm in the load zone. The moment the fourth arm enters the load zone after arm A turns 60°, there is a load sharing by this fourth arm. The dynamic equilibrium of the system gets disturbed. This load sharing leads to the fact that the resultant of frictional forces is not passing through A. During the further motion of the arm, this unbalanced couple increases and is maximum at around 150°. When A is at 150°, E is at 30° and F is at 90°, the load is shared by three arms and no other arm is near to its entry into the load zone, nor at the exit of the load zone. The maximum value of unbalanced couple is attributed to this reason. Then the arm D enters the load zone and A start it exit from the load zone. When A is at 180°, arm D enters the load zone and we have four arms to share the load. This leads to lowering the value of unbalanced couple from 150° to 180°. After 180–190°, there is again the presence of this unbalanced couple but its values are small.

8. Conclusions

1. The current design criterion of flat belt drive pulley on the basis that half the arms take the load appears true practically. This is because; the factor of safety is very high, of the order of 8.

Owing to limitations of casting process, the rim cannot be made thin. Hence rim thickness is more than what is assumed, the armload variation less than predicted. With the hypothesis stated in problem formulation, we found that the factor of safety is in the range of 8–10. So current design is an over design.

2. The arm vibrations resulting in arm failure is not reported from industry. The reason is that the system, even though subjected to varying load, as discussed in first and second approach, settles quickly. As per the first approach, it is a classic example of Posicast Control System [12].
3. As discussed in second approach, the arm is subjected to varying load and there is a presence of unbalanced couple at the arm–rim interface. This unbalanced couple leads to phenomenon of belt flutter, which is observed commonly.
4. This study gives us cursory idea of stress under vibration of the arm and nature of armload variation.
5. By this study a new avenue of analyzing the flat belt drive pulley is suggested and the comparative results of both approaches suggests that second approach is more refined than the first approach [12].

9. Scope of future work

The results of these two approaches can be compared with the third approach using FEM as discussed in Section 2.3 and then experimentally verified [35,36]. This work is in progress.

Appendix A

The quantities K_1 to K_{26} are given by following equations:

$$K_1 = a_0 - (2a_2/\omega_n^2) + (24a_4/\omega_n^4) - (720/\omega_n^6), \tag{A.1}$$

$$K_2 = a_1 + a_2 - (6a_3/\omega_n^2) + (120a_5/\omega_n^4), \tag{A.2}$$

$$K_3 = (-12a_4/\omega_n^2) + (360a_6/\omega_n^4), \tag{A.3}$$

$$K_4 = a_3 - (20a_5/\omega_n^2), \tag{A.4}$$

$$K_5 = a_4 - (30a_6/\omega_n^2), \tag{A.5}$$

$$K_6 = a_5, \tag{A.6}$$

$$K_7 = a_6, \tag{A.7}$$

$$K_8 = a_1 - (6a_3/\omega_n^2) + (120a_5/\omega_n^4), \tag{A.8}$$

$$K_9 = 2a_2 - (24a_4/\omega_n^2) + (720a_6/\omega_n^4), \tag{A.9}$$

$$K_{10} = 3a_3 - (60a_5/\omega_n^2), \tag{A.10}$$

$$K_{11} = 4a_4 - (120a_6/\omega_n^2), \tag{A.11}$$

$$K_{12} = 5a_5, \tag{A.12}$$

$$K_{13} = 6a_6, \tag{A.13}$$

$$K_{14} = (-a_0 + (2*a_2/\omega_n^2) - (24a_4/\omega_n^4) + (720a_6/\omega_n^6)), \tag{A.14}$$

$$K_{15} = (-a_1 + (6a_3/\omega_n^2) - (120a_5/\omega_n^4)), \tag{A.15}$$

$$K_{16} = (-a_2 + (12a_4/\omega_n^2) - (360a_6/\omega_n^4)), \tag{A.16}$$

$$K_{17} = (-a_3 + 20a_5/\omega_n^2), \tag{A.17}$$

$$K_{18} = (-a_4 + 30a_6), \tag{A.18}$$

$$K_{19} = (-a_5), \tag{A.19}$$

$$K_{20} = (-a_6), \tag{A.20}$$

$$K_{21} = (a_1 - (6a_3/\omega_n^2) + (120a_5/\omega_n^4)), \tag{A.21}$$

$$K_{22} = 2a_2 - (24a_4/\omega_n^2) + (720a_6/\omega_n^4)), \tag{A.22}$$

$$K_{23} = (3a_2 - 60(a_5/\omega_n^2)), \tag{A.23}$$

$$K_{24} = (4a_4 - (120a_6/\omega_n^2)), \tag{A.24}$$

$$K_{25} = 5a_5, \tag{A.25}$$

$$K_{26} = 6a_6. \tag{A.26}$$

Appendix B. Algorithm: Approach_2

VARIABLE DEFINITION
FLOAT
T2/tension in slack side
Lap/angle of lap
xsum, ysum, sum /variables used in program to collect the sum
dphi/dphi = (phi/d), Angle of lap under consideration at dth part of total angle turn
theta/final value of angle of lap in the load zone under consideration
dtheta = (turn*PI/180)-angle made by resultant frictional force with respect to line OA
turn/ Angle considered for iteration out of total angle 'lap'
d/number of divisions of angle of iteration
j/intermediate variable
n/rpm of pulley

t/any time instant
period/time taken for one revolution of pulley
phi/phi = turn*PI/180
aload/normal component of armload
xr, yr/resultant frictional forces in x and y direction respectively
tload/tangential component of armload
dtheta/small angle out of ''turn'' considered for iteration
x/distance between the resultant of frictional forces and A
ft/equivalent load of the couple
force/x-component of resultant force
couple/unbalance couple
p/total tangential load
dd,ss/intermediate variables in algorithm
ps/stress in arm
sut/ultimate tensile strength of material
h/average value of major axis of elliptical cross section
mu/coefficient of friction between pulley and belt
tu1, tu2/range of variable ''turn''
di1, di2/range of number of divisions of each ''turn''
dturn/intermediate variable
st [20]/counter to change variable ''turn''

FILE DEFINITION

FILE*fp1;

CONSTANT DEFINITION

$E = 2.71829, PI = 3.1415926$

STRUCTURE

```
    {
        float df[4]
        float xcomp[4]
        float ycomp[4]
        float resf
        float restheta
    }f,temp
```

Step 1 [Read input parameters from keyboard]

```
READ (t2, lap, mu, n, sut, h, tu1, tu2, di1, di2)
```

Step 2 [For the first region in the load zone when four arm are present in it]

```
period = 60/n
for(dturn=tu1;dturn<=tu2;dturn++)
    {
    for(d=di1;d<=di2;d++)
            for(turn=dturn;turn<=(lap-180);turn+=dturn)
                {
                    phi = turn*PI/180
             for(dphi=(phi/d),j=0;j<=3;dphi+=(phi/d),j++)
             {
              sum = sum + (dphi - phi/d)
```

```
                f.df[j] = mu * t2*pow(E,(mu*(sum+dhpi/2)))*dphi
        }
         sum=0
         for(theta=(phi/(d*2)),j=0;j<=3;theta+=(phi/d),j++)
           {
            f.xcomp[j] =  f.df[j]*cos(theta)
            f.ycomp[j] =  f.df[j]*sin(theta)
            xsum += f.xcomp[j]
            ysum += f.ycomp[j]
           }
         f.resf = pow((xsum*xsum + ysum*ysum),0.5)
         f.restheta = atan(ysum/xsum)
         aload = f.resf*sin(f.restheta)[normal component]
         tload = f.resf*cos(f.restheta)[tangential component]
         t = period * turn / 360
         dtheta=(turn*PI/180)-f.restheta
         x = l*abs(dtheta)*tan(abs(dtheta))
         force = f.resf*cos(abs(dtheta))
         couple = force*x [Unbalanced Couple]
         ft=couple/(l)
         p=tload+ft [Total Load Acting on Arm to Find Stress]
         dd= (32*p*l/(3.14*h*h*h)+4*aload/(3.14*h*h))
         ss= 32*aload/(3*3.14*h*h)
         ps=dd+sqrt(dd*dd+ss*ss)[Stress Under Vibration]
         WRITE_FILE(fp1,"",t,aload,tload,couple,p,ps)
           xsum=0
           ysum=0
      }
  CLOSE_FILE(fp1)
   }
   st[dturn]=turn;
 }
```

Step 3 [For the second region in the load zone when three arms are present in it]

```
                for(dturn=tu1;dturn<=tu2;dturn++)
  {
  for(d=di1;d<=di2;d++)
  {
                  fp1=OPEN_FILE(name,"w")
 for(turn=st[dturn];turn<=60;turn+=dturn)
   {
     phi=turn*PI/180
     for(dphi=(phi/d),j=0;j<=3;dphi+=(phi/d),j++)
        {
           sum = sum + (dphi - phi/d)
           f.df[j] = mu * t2 * pow(E,(mu*(sum+dphi/2)))*dphi
        }
        sum  =0
     for(theta=(phi/(d*2)),j=0;j<=3;theta+=(phi/d),j++)
        {
           f.xcomp[j] =  f.df[j]*cos(theta)
```

```
            f.ycomp[j] =  f.df[j]*sin(theta)
            xsum += f.xcomp[j]
            ysum += f.ycomp[j]
        }
    f.resf = pow((xsum*xsum + ysum*ysum),0.5)
    f.restheta = atan(ysum/xsum)
    xsum=0
    ysum=0
    for(dphi=PI/(3*d),j=0;j<=3;dphi+=PI/(3*d),j++)
       {
          sum = sum + (dphi - PI/(3*d))
          temp.df[j]=mu*t2*pow(E,(mu*(phi+sum+dphi/2)))*dphi
       }
       sum  =0
    for(theta=PI/(6*d),j=0;j<=3;theta+=PI/(3*d),j++)
       {
        temp.xcomp[j] =  temp.df[j]*cos(theta)              temp.ycomp[j] =
        temp.df[j]*sin(theta)
        xsum += temp.xcomp[j]
        ysum += temp.ycomp[j]
       }
    temp.resf = pow((xsum*xsum + ysum*ysum),0.5)
    temp.restheta = atan(ysum/xsum)
  xr=f.resf*cos(f.restheta)+emp.resf*cos((temp.restheta+phi))
yr=f.resf*sin(f.restheta)+temp.resf*sin((temp.restheta+phi))
    f.resf = pow((xr*xr + yr*yr),0.5)
    f.restheta = atan(yr/xr)
    aload = f.resf*sin(f.restheta)
    tload = f.resf*cos(f.restheta)
    t = period * turn / 360
    dtheta=(turn*PI/180)-f.restheta
    x = l*abs(dtheta)*tan(abs(dtheta))
    force = f.resf*cos(abs(dtheta))
    couple = force*x
    ft=couple/(l)
        p=tload+ft
        dd= (32*p*l/(3.14*h*h*h)+4*aload/(3.14*h*h))
        ss= 32*aload/(3*3.14*h*h)
        ps=dd+sqrt(dd*dd+ss*ss)
        WRITE_FILE(fp1,"", t,aload,tload,couple,p,ps)
    xsum = 0
    ysum = 0
     }
  CLOSE_FILE(fp1)
   }
   st[dturn]=turn
 }
```

Step 4 [For the third region in the load zone when four arms are present in it]

```
                for(dturn=tu1;dturn<=tu2;dturn++)
                 {
```

```
 for(d=di1;d<=di2;d++)
   {
       fp1=OPEN_FILE(nam  e,"w")
for(turn=st[dturn];turn<=(120+(lap-180));turn+=dturn)
    {
     phi = (turn-60)*PI/180
     for(dphi=PI/(3*d),j=0;j<=3;dphi+=PI/(3*d),j++)
        {
           sum = sum + (dphi - PI/(3*d))
           f.df[j]=mu*t2*pow(E,(mu*(phi+sum+dphi/2)))*dphi
        }
        sum  =0
     for(theta=PI/(6*d),j=0;j<=3;theta+=PI/(3*d),j++)
        {
           f.xcomp[j] =  f.df[j]*cos(theta)
           f.ycomp[j] =  f.df[j]*sin(theta)
           xsum += f.xcomp[j]
           ysum += f.ycomp[j]
        }
     f.resf = pow((xsum*xsum + ysum*ysum),0.5)
     f.restheta = atan(ysum/xsum)
     aload = f.resf*sin(f.restheta)
     tload = f.resf*cos(f.restheta)
     t = period * turn / 360
     dtheta=(turn*PI/180)-f.restheta
     x = l*abs(dtheta)*tan(abs(dtheta))
     force = f.resf*cos(abs(dtheta))
     couple = force*x
     ft=couple/(l)
          p=tload+ft
          dd= (32*p*l/(3.14*h*h*h)+4*aload/(3.14*h*h))
          ss= 32*aload/(3*3.14*h*h)
          ps=dd+sqrt(dd*dd+ss*ss)
     WRITE_FILE(fp6,"    ",t,aload,tload,couple,p,ps)
     xsum=0
     ysum=0
     }
  CLOSE_FILE(fp1)
    }
   st[dturn]=turn
 }
```

Step 5 [For the fourth region in the load zone when three arms are present in it]

```
                for(dturn=tu1;dturn<=tu2;dturn++)
                 { for(d=di1;d<=di2;d++)
    {
          fp1=OPEN_FILE(name,"w")
  for(turn=st[dturn];turn<=180;turn+=dturn)
    {
         phi = (lap-turn)*PI/180
    for(dphi=phi/d,j=0;j<=3;dphi+=phi/d,j++)
```

```
        {
            sum = sum + (dphi - phi/d)
f.df[j]=mu*t2*pow(E,(mu*((turn*PI/180)+sum+dphi/2)))*dphi      }
        sum  =0
     for(theta=phi/(d*2),j=0;j<=3;theta+=phi/d,j++)
        {
            f.xcomp[j] =  f.df[j]*cos(theta)
            f.ycomp[j] =  f.df[j]*sin(theta)
            xsum += f.xcomp[j]
            ysum += f.ycomp[j]
        }
     f.resf = pow((xsum*xsum + ysum*ysum),0.5)
     f.restheta = atan(ysum/xsum)
     aload = f.resf*sin(f.restheta)
     tload = f.resf*cos(f.restheta)
     t = period * turn / 360
     dtheta=(turn*PI/180)-f.restheta
     x = l*abs(dtheta)*tan(abs(dtheta))
     force = f.resf*cos(abs(dtheta))
     couple = force*x
     ft=couple/(l)
          p=tload+ft
          dd= (32*p*l/(3.14*h*h*h)+4*aload/(3.14*h*h))
          ss= 32*aload/(3*3.14*h*h)
          ps=dd+sqrt(dd*dd+ss*ss)
     WRITE_FILE(fp1,"       ",t,aload,tload,couple,p,ps)
     xsum=0
     ysum=0
     }
  CLOSE_FILE(fp1)
   }
   st[dturn]=turn
 }
```

Step 6 [For the fifth region in the load zone when four arms are present in it]

```
for(dturn=tu1;dturn<=tu2;dturn++)
  {
    for(d=di1;d<=di2;d++)
    {
        fp1=OPEN_FILE(nam  e,"w")
      for(turn=st[dturn];turn<=lap;turn+=dturn)
       {
       phi=(turn-60)*PI/180
       for(dphi=PI/(3*d),j=0;j<=3;dphi+=PI/(3*d),j++)
            {
             sum = sum + (dphi - PI/12)
             f.df[j]=mu*t2*pow(E,(mu*(phi+sum+dphi/2)))*dphi
            }
           sum=0
      for(theta=PI/(6*d),j=0;j<=3;theta+=PI/(3*d),j++)
            {
             f.xcomp[j] =  f.df[j]*cos(theta)
```

```
            f.ycomp[j] =  f.df[j]*sin(theta)
            xsum += f.xcomp[j]
            ysum += f.ycomp[j]
           }
     f.resf = pow((xsum*xsum + ysum*ysum),0.5)
     f.restheta = atan(ysum/xsum)
     xsum=0
     ysum=0
     phi = (lap-turn)*PI/180;
     for(dphi=phi/d,j=0;j<=3;dphi+=phi/d,j++)
        {
            sum = sum + (dphi - phi/d)
temp.df[j]=mu*t2*pow(E,(mu*((turn*PI/180)+sum+dphi/2)))*dphi
        }
        sum  =0
     for(theta=phi/(d*2),j=0;j<=3;theta+=phi/d,j++)
        {
            temp.xcomp[j] =  temp.df[j]*cos(theta)
            temp.ycomp[j] =  temp.df[j]*sin(theta)
            xsum += temp.xcomp[j]
            ysum += temp.ycomp[j]
        }
     temp.resf = pow((xsum*xsum + ysum*ysum),0.5)
     temp.restheta = atan(ysum/xsum)
xr=f.resf*cos(f.restheta)+temp.resf*cos((temp.restheta+PI/3))
yr=f.resf*sin(f.restheta)+temp.resf*sin((temp.restheta+PI/3))
     f.resf = pow((xr*xr + yr*yr),0.5)
     f.restheta = atan(yr/xr)
     aload = f.resf*sin(f.restheta)
     tload = f.resf*cos(f.restheta)
     t = period * turn / 360
     dtheta=(turn*PI/180)-f.restheta
     x = l*abs(dtheta)*tan(abs(dtheta))
     force = f.resf*cos(abs(dtheta))
     couple = force*x
     ft=couple/(l)
          p=tload+ft
          dd= (32*p*l/(3.14*h*h*h)+4*aload/(3.14*h*h))
          ss= 32*aload/(3*3.14*h*h)
          ps=dd+sqrt(dd*dd+ss*ss)
     WRITE_FILE(fp1,"",t,aload,tload,couple,p,ps)
     xsum=0
     ysum=0
     }
    CLOSE_FILE(fp1)
   }
   }
Step 7 [Should be same as Step 5]
Step 8 [Should be same as Step 4]
  }
```

Appendix C. Nomenclature

$a_0, a_1, \ldots, a_6$	coefficients of polynomial equation of f
C	center distance, m
C_{unbal}	unbalanced couple, N m
C_{eq}	equivalent viscous damping
C_b	reaction couple provided by the belt on the rim, N m
C_l	reaction couple provided by the remaining portion of the lamina on the portion of lamina under consideration, N m
D	number of divisions of the angle 'turn' done to perform the iteration
D_1	diameter of smaller pulley, m
D_2	diameter of larger pulley, m
E	modulus of elasticity of the pulley material, N/mm^2
δF_f	elemental frictional force, N
δF_{fi}	elemental frictional force at an angle $\delta\phi_i$ from line of symmetry 01 as shown in Fig. 4, N
$\sum F_f$	resultant frictional force, N
F_c	equal and opposite force applied at A equal to $\sum F_f$, N
F_{ca}	centrifugal force acting on the arm, N
F_{cr}	centrifugal force acting on the rim, N
F_{tan}	tangential component of resultant frictional force, N
F_{nor}	normal component of resultant frictional force, N
F_a	reaction of the arm OA at A
F	force acting on the arm considered equal to $F(t)$, N
$F(t)$	arm load at any instant of time t, N
F_{couple}	force calculated by transferring the unbalanced couple C_{unbal} to an equivalent force system of two equal and opposite forces separated by distance l_{couple}, N
F_{s1}, F_{s2}	shear forces acting on the lamina under consideration due to remaining portion of lamina, N
F_{rl}, F_{rr}	tensile forces acting on the lamina under consideration due to left and right side of the remaining rim portion, N
F_{dy}	equivalent dynamic load acting on the arm
I	moment of inertia of the arm cross-section, m^4
impulse	$(f\ \mathrm{d}t_i)$ is termed as impulse
K_{eq}	equivalent spring stiffness, N/m
$K_1 \ldots K_{26}$	constants in equation of $\times$ (40) explained in Appendix A
Lap	total angle of lap of the pulley, rad
L	length of the arm, m
l_{couple}	couple arm, m
M_{eq}	equivalent mass of the arm of the pulley, kg
M	mass of the arm of the pulley, kg
P	power transmitted, W
R	radius of the pulley, mm
Rn	reaction of the arm on the rim, N

r_g	distance of center of mass of arm of pulley from hub, m
turn	angle considered for iteration out of total angle 'lap'
T	the tension in the belt at any angle of ϕ from the line of symmetry 01 in Fig. 1, N (Eq. (2))
t_1, t_2, t_3	time instances of positions of arms in the load zones, sec
t_i	time at which the impulse ($f\,\mathrm{d}t_i$) is applied and is a variation in the equation
t	time at which we observe the system
T_s	tension on loose side, N
T_t	tension on tight side, N
X	unbalanced couple arm, m
X	deflection of the arm, m
Z	section modulus of the arm, m^3
ϕ	angle of lap or contact, rad
ω_n	natural frequency of the arm, rad/s
ϕ_i	active angle of the lap at any instant of time t, rad
$\delta\phi_i$	angle of lap under consideration at ith part of total angle turn, rad
σ_{arm}	stress under vibration induced in the arm of the pulley, MPa
$\angle 104$	angle of lap in the active load zone, rad (Fig. 5)
μ	coefficient of friction (for belt-pulley surface)
ξ	damping coefficient

References

[1] J.E. Shigley, L.D. Mitchell, *Mechanical Engineering Design*, McGraw-Hill, Tokyo, 1983.
[2] T.C. Firbank, Mechanics of Flat Belt Drive, *International Journal of Mechanical Science* 12 (1970) 1053–1063.
[3] L.M. Valadimin, J.B. Hartman, *Machine Design*, CBS Publisher, Delhi, 1983.
[4] E.W. Stanton, *Machine Design*, D.B. Taraporwala, Mumbai (India), 1965.
[5] L.S. Mark, *Mechanical Engineers Handbook*, McGraw-Hill, New York, 1950.
[6] B.D. Shiwalkar, *Design Data for Machine Elements*, Central Techno Publishers, Nagpur, 1999.
[7] T.N. Restinov, *Machine Design*, Mir Publications, Moscow, 1984.
[8] Pandya, Shah, *Machine Design*, Dhanpat Rai and Co., New Delhi, 1990.
[9] K. Lingaiyah, *Machine Design Handbook*, McGraw-Hill, New York, 1994.
[10] Rothbert, *Standard Handbook of Machine Design*, McGraw-Hill, New York, 1994.
[11] J.P. Modak, et al., Load variation of the arm of the belt drive pulleys, *Proceedings of Eighth World Congress on the Theory of Machines and Mechanisms*, Prague, Czechoslovakia, 1990, pp. 87–90.
[12] P.M. Singru, J.P. Modak, Computer simulation of dynamic and vibration response of arm of belt drive pulley, *Journal of Sound and Vibration* 242 (2) (2001) 277–293.
[13] S. Abrate, Vibrations of belts and belt drives, *Mechanisms and Machine Theory* 27 (6) (1992) 645–659.
[14] M. Saraph, A. Midha, J.C. Wambold, Stress analysis of mechanical sheaves and pulleys, *Transactions of American Society of Mechanical Engineers Journal of Mechanism, Transmission and Automation in Design* 105 (1983) 400–406.
[15] H. Belofsky, On the theory of power transmission by a flat, elastic belt, *Wear* 25 (1973) 73–84.
[16] H. Kim, K.M. Marshek, Effect of belt velocity on flat belt drive behavior, *Mechanisms and Machine Theory* 22 (1) (1987) 523–527.
[17] H. Kim, M. Naji, K.M. Marshek, Forces between an abrasive belt and pulley, *Mechanisms and Machine Theory* 22 (1) (1987) 97–103.

[18] R.V. Virabov, Effect of centrifugal forces on behaviour of belt drive, *Russian Engineering Journal* XLVI (11) (1966) 22–26.
[19] L. Zhang, J.W. Zu, One-to-one auto-parametric resonance in serpentine belt drive systems, *Journal of Sound and Vibration* 232 (4) (2000) 783–806.
[20] Y.I. Kwon, J.G. Ih, Vibrational power flow in the moving belt passing through a tensioner, *Journal of Sound and Vibration* 229 (2) (2000) 329–353.
[21] F. Pellicano, A. Fregolent, A. Bertuzzi, F. Vestroni, Primary and parametric nonlinear resonances of a power transmission belt: experimental and theoretical analysis, *Journal of Sound and Vibration* 244 (4) (2001) 669–684.
[22] T. Iwatsubo, K. Hasengawa, S. Arii, K. Shiohata, The formulation of dynamic analysis of a multiple belt system, *Journal of Sound and Vibration* 205 (3) (1997) 293–307.
[23] J. Moon, W. Wickert, Radial boundary vibration of misaligned v-belt drives, *Journal of Sound and Vibration* 225 (3) (1999) 527–541.
[24] L. Zhang, J.W. Zu, Modal analysis of serpentine belt drive system, *Journal of Sound and Vibration* 222 (2) (1999) 259–279.
[25] Wan-Teck Rim, Kwang-Joon Kim, Identification of tension in a belt drive system analysing flexural vibration, *Mechanical Systems and Signal Processing* 8 (2) (1994) 199–213.
[26] K.S. Kim, M.J. Lee, Analysis of the nonlinear vibration characteristics of a belt driven system, *Journal of Sound and Vibration* 223 (5) (1999) 723–740.
[27] P.M. Singru, et al., Computer aided design of mechanical systems, *Proceedings of National Seminar on Emerging Trends in Design Engineering*, M.N.R.E.C., Allahabad, 1997, pp. I26–I36.
[28] P.M. Singru, et al., Computer aided design of mechanical systems (CADOMS) ver. 3.0, *National Conference on Intelligent Manufacturing Systems*, C.I.T., Coimbatore, 1998, pp. D1.1-D1.8.
[29] P.M. Singru, *Manual of CADOM*, unpublished.
[30] P.M. Singru, A. Alias, Computer aided design of machines, *Proceedings of First International Conference on Intelligent Flexible Autonomous Manufacturing Systems*, C.I.T., Coimbatore (India), 2000.
[31] J.E. Shigley, J.J. Uicker Jr., *Theory of Machines and Mechanisms*, McGraw-Hill, Tokyo, 1981.
[32] W.T. Thomson, *Theory of Vibration with Applications*, CBS Publication, Delhi, 1988.
[33] J.S. Rao, *Advanced Theory of Vibration*, Wiley Eastern Publication, New Delhi, 1986.
[34] B.J. Lazen, *Damping of Materials and Members in Structural Mechanics*, Pergamon Press, London, 1968.
[35] P.M. Singru, J.P. Modak, Proposed experimental setup for studying dynamic and vibration response of belt drive pulley, *Proceedings of the National Symposium on Recent Advances in Experimental Mechanics*, Organized by Indian Institute of Technology, Kanpur, 2000, pp. 29–35.
[36] P.M. Singru, J.P. Modak, Dynamic stress analysis of the arms of the belt drive pulley using finite element method, *Proceedings of the National Conference on Industrial Problems in Machines and Mechanisms*, Organized by Priyadarshini College of Engineering and Architecture, Nagpur, 2000, pp. 84–90.